Discover Oncology

Analysis

Systematic analysis of the aberrances and functional implications of epigenetic genes in hepatocellular carcinoma

Jiehua Zheng[1] · Weixun Lin[1] · Jing Tang[2] · Bo Xu[1]

Received: 20 October 2024 / Accepted: 20 May 2025
Published online: 27 May 2025

Abstract
Epigenetic alteration leads to the aberrant transcriptional programmes that faciliate cancer onset and progression. In-depth understanding of the epigenetic alteration of cancers is critical for crucial in developing meaningful cancer treatment that may provide a meaningful improvement in overall survival. Based on the data in The Cancer Genome Atlas (TCGA), we performed a comprehensive and systematic genomic study of epigenetic genes. We defined the epigenetic score to reveal the functional roles of epigenetic genes. We found that epigenetic score was higher in tumors than in normal tissues in most cancers and was associated with poorer prognosis, especially in hepatocellular carcinoma (HCC).Our study also found that epigenetic score is significantly related to immune evasion in HCC. To guide efficient pharmalogical intervention of unfolded protein response to help patients, we performed virtual screening and found some compounds targeting UHRF1 could become a good pharmaceutical therapeutic candidate in unique or adjuvant therapeutic approaches toward HCC.

Keywords Epigenetic regulator · Pancancer · Genomic study · Bioinformatics · Virtual screening

Abbreviations

HCC	Hepatocellular Carcinoma
HBV	Hepatitis B Virus
HCV	Hepatitis C Virus
NAFLD	Non-Alcoholic Fatty Liver Disease
ERRG	Epigenetic Regulation-Related Gene
LIHC	Liver Hepatocellular Carcinoma
ssGSEA	Single-Sample Gene Set Enrichment Analysis
SCNA	Somatic Copy-Number Alteration
SNV	Single Nucleotide Variation
GO	Gene Ontology
GSVA	Gene Set Variation Analysis

Jiehua Zheng and Weixun Lin have contributed equally to this work and should be considered co-first authors.

Supplementary Information The online version contains supplementary material available at https://doi.org/10.1007/s12672-025-02765-z.

✉ Bo Xu, aabb97@163.com | [1]Department of General Surgery, The First Affiliated Hospital of Jinan University, No. 601, Huangpu Avenue, Guangzhou 510632, Guangdong, People's Republic of China. [2]Department of Thyroid and Breast Surgery, Shenzhen Second People's Hospital, Shenzhen, Guangdong, China.

ROC	Receiver Operating Characteristic
NES	Normalized Enrichment Score
TAMs	Tumor-Associated Macrophages
SPP1	Secreted Phosphoprotein 1
PD-L1	Programmed Death-Ligand 1
TIDE	Tumor Immune Dysfunction and Exclusion
PDB	Protein Data Bank
FDA	Food and Drug Administration
UMAP	Uniform Manifold Approximation and Projection

1 Introduction

Genetic and epigenetic alterations in DNA, such as DNA methylation and histone modifications, play important roles in the regulation of tumor gene expression. These alterations are closely associated with the acquisition of malignant progression and biochemical aberrations [1, 2]. To reverse the progress has became an promising treatment in oncotherapy [3]. Up to now, various FDA approval drugs targeting epigenetic alterations such as DNA methyltransferase inhibitors and histone deacetylase inhibitors has generated forefront clinical practice [4].

As the understanding of epigenetic alteration has increased, its oncogenic effects has been disclosed. Emerging evidences indicate that cancer drug resistance, which contributed to tumour aggressiveness, are closely related to the aberrant chromatin landscape and the epigenetic alteration orchestrate the specific inhibited phenotype [5–7]. In combination with epigenetic regimens could be more effective than any single traditional antineoplaston [8]. In addition, cancer cells are ordinarily hijack varieties of epigenetic factors to escape immunological surveillance by facilitating the production of immunomodulatory cytokines or regulating the activation of immune checkpoint [9].

Moreover, the reversion of epigenetic alteration is able to restrain the uncontrolled cancer cell growth and the acquisition of tumor malignant phenotype [10]. Therefore, pharmaceutical modulation of epigenetic regulators could result in novel and efficient anticancer therapies.

Liver cancer is one of the leading causes of cancer-related deaths worldwide, with hepatocellular carcinoma (HCC) accounting for approximately 75–85% of all primary liver cancer cases. HCC is a highly aggressive malignancy often associated with chronic liver diseases, such as hepatitis B virus (HBV) and hepatitis C virus (HCV) infections, as well as non-viral factors like alcohol consumption and non-alcoholic fatty liver disease (NAFLD) [11]. Despite advances in diagnostic and therapeutic strategies, the prognosis of HCC remains poor due to its late diagnosis, high recurrence rate, and resistance to conventional therapies. Understanding the molecular mechanisms underlying HCC progression, including genetic and epigenetic alterations, is crucial for developing novel therapeutic approaches [12].

Herein, we first performed cox analysis of epigenetic regulated related genes (ERRG) and found that ERRG may play an important role in Liver hepatocellular carcinoma (LIHC). To further understand the role of ERRG across different cancers. Epigenetic score, we use the 23 genes of ERRGs with highest cox rank to define an epigenetic score and performed a comprehensive analysis in LIHC. These results highlight the critical roles of epigenetic regulated related genes in LIHC and should be helpful for further researches of epigenetic-related molecular mechanisms and pharmacological therapy development.

2 Methods

2.1 Data acquisition

All data of this article comes from public databases that is freely available.

148 epigenetic regulation related genes were obtained from reactome pathways (R-HSA-212165) which downloaded from website of Gene Set Enrichment Analysis (GSEA) (http://www.gseamsigdb.org/gsea/index.jsp). And 142 epigenetic regulation relative gene list (Table S1) were selected in our study (6 of the 148 genes are not in our pancancer expression matrix).

The pancancer mRNA expression data and clinical data with follow-up were downloaded from National Cancer Institute Cancer Research Genomic Data Commons (GDC) (https://gdc.cancer.gov/about-data/publications/pancanatlas).

CIBERSORT immune fractions and Scores for 160 Genes Signatures in Tumor Samples were downloaded from GDC (https://gdc.cancer.gov/about-data/publications). The Cancer Genome Atlas (TCGA) LIHC Phenotypes data was obtained from xena website (https:// xenabrowser.net/datapages/). The pan-cancer ssGSEA scores for 1387 constituent PARADIGM algorithm integrates pathway was obtained from xena website. The Gene Expression Omnibus (GEO) database (http://www.ncbi.nlm.nih.gov/geo/) was explored, and GSE14520 gene expression dataset was downloaded for this study. Mutation data of LIHC was downloaded from cBioPortal database (http://www.cbioportal.org/datasets). Gene expression profile of exosome was downloaded from BBcancer database (http://bbcancer.renlab.org/download).

2.2 Differential expression analysis of mRNA

Differentially Expression analysis was calculated by the 'limma' R package to identify the differentially expressed mRNA with *p*-value less than 0.05. epigenetic score difference between cancer and normal tissue was also calculated by the 'limma' R package.

2.3 Somatic copy-number alteration (SCNA) and single nucleotide variation (SNV) analysis

Copy-number alteration of each gene were calculated via the heterozygosity and homozygosity of amplification and deletion, in which over five percent was regarded as high-frequency SCNA. The mutation and CNA events were integrated, while only homozygous amplification and deletion were included, and only protein-coding mutations were retained. For each cancer type, the genes were considered to be mutually exclusive if they had a q value of 0.05. SNV datawere collected across 16 cancer types from the TCGA database. SNV mutation frequency (percentage) of each gene's coding region was calculated using the formula: Number of Mutated Samples/Number of Cancer Samples. An SNV oncoplot plot was generated using the R package "maftools".

2.4 Pathway enrichment

GSVA pathway analyses were primarily performed on the hallmark pathways described in online website 'gsea-msigdb' (http://www.gsea-msigdb.org/gsea/index.jsp) and exported using the GSEABase package. To reduce pathway overlaps, we applied gene set trimmed method and GSVA analyses method described in the article. R package 'GSVA' was applied. GO enrichment was using 'GOplot' R and 'clusterProfiler' R package.

2.5 Calculated the epigenetic score

The index to represent the risky epigenetic regulation related genes level was establish based on the expression data from TCGA LIHC dataset of these genes, which were selected via multivariate logistic regression. The 23 genes were the independent risk factors in LIHC, which were listed in Table S4.The enrichment score (ES) of gene set was calculated using single sample gene set enrichment analysis (ssGSEA) in the R package 'GSVA', and the normalized ES was defined as the Epigenetic Score to computationally dissect the risky epigenetic regulation trends of the tissue samples.

2.6 Bioinformatics analysis of ScRNA-seq data and ST-RNA-seq data

ScRNA-seq data of HCC patients was obtained from the National Center for Biotechnology Information Gene Expression Omnibus (NCBI GEO; accession number GSE156337). The spatial transcriptomics data were acquired from the following hyperlinks: http://lifeome.net/supp/livercancer-st/data.htm. For scRNA-seq and ST-RNA-seq analysis, the primary tool used was the 'Seurat' R package (version 4.0.2). Post preprocessing, cell clusters were referred to the original article and visualised them using 'DimPlot' functions. Target genes analyses were visualised using UMAP plots ('FeaturePlot'), heatmaps ('DoHeatmap') and violin plots ('VlnPlot'). Malignant cell quantification of spatial transcriptomics was using R package SpaCET and a demo workflow to reproduce our main results are available at GitHub (https://www.github.com/data2intelligence/SpaCET).

2.7 Virtual screening to find potential pharmacological intervention towards UHRF1

Protein structure of UHRF1 was found from the the Protein Data Bank (PDB; http://www.rcsb.org/pdb/). Schrödinger software was applied to prepared for virtual screening with hydrogen atoms and charges added. Compounds obtained from the FDA small molecules database and filtered by Lipinski's rule-of-five and Veber rule. And then the rest compounds were put into Schrödinger software and LigPrep module and Epik program was used for preparation (using OPLS_2005 force field); Active pocket was found using SiteMap module of Schrödinger software. Pan assay interference compounds (PAINS) was identified and filtered by Canvas 1.1. QikProp 3.2 program of Schrödinger software was used for filtration through 'Lipinski rule of five'. All compounds were docked into the active site by applying Glide SP (Standard precision) and XP (Extra precision) docking methods.

2.8 Statistical analysis

Main statistical tests were performed in R statistical software (Version 4.0.2, R Core Team, R Foundation for Statistical Computing, Vienna, Austria) and RStudio (Version 1.3.1073). Figures 4C and 6A were visualized by GraphPad Prism 8 and test by Chi-squre. Comparison of a variable in two or more than two groups was performed using nonparametric test (Wilcoxon rank-sum test or Kruskal–Wallis test). Correlation between two continuous variables was measured by Spearman's rank-order correlation. Kaplan–Meier survival analysis was using 'survival' and 'survminer' R package. For all statistical analysis, a two-tailed $p < 0.05$ was considered significant.

3 Results

3.1 General pancancer status of epigenetic regulation related genes across cancer types

We first performed univariate Cox regression to screen epigenetic regulation related genes across the 30 cancer types. All of the epigenetic regulation related genes correlate with patient overall survival in at least one type of cancer (Fig. 1A). Risky score was defined as follow: The genes expression significantly associated with worse and better survival were assigned a score of positive one score and negative one score respectively. The risky score of each cancer was the total cox score of all the epigenetic regulation related genes (Table S2) and shown as Fig. 1B in descending order. The risky score of each gene was the total cox score of each gene across different cancer types (Table S3) and shown as Fig. 1C in descending order. We found that LIHC has the highest risky score across different cancer types and UHRF1 has the highest risky score across different cancer types. The 24 genes with highest score (Fig. 1C) including UHRF1, ACTB, DNMT3B, TAF1A, CBX3, EZH2, TDG, EED, PHF19, SUV39H1, DDX21, MYBBP1A, SAP30, TAF1D, CDK7, DNMT1, DNMT3A, GSK3B, GTF2H5, HDAC2, MBD2, POLR2H, POLR2K and TET1, were selected for further analysis.

Futhermore, gene expression differences between cancer and normal tissue of the twenty-four epigenetic regulation related genes with highest risky score were analyzed in sixteen different cancer types and the other 14 cancers out of the total 30 cancer types which have no normal tissue data were removed in the analysis. We found that all the 24 genes were differentially expressed in most cancers (Fig. 2A).

As somatic copy number alterations (SCNA) is common in cancers which was one of the important factor affecting the genetic aberration, we futher investigate the SCNA across cancers and the results indicated the general SCNA occurred at high frequencies in most cancer types (Fig. 2B). Besides, we also analyzed epigenetic regulation related SNP data to detect the frequency and variant types across different cancer types.

As shown in Figure S1A, the SNV frequency of the 24 genes was 41.91% (782 of 1866 samples). Variant type analysis showed that missense mutations were the main SNP type. SNV percentage analysis indicated that the top 5 mutated genes were TET1, DNMT3A, DNMT1, DNMT3B, MYBBP1A,of which the mutation percentages were 9, 6, 6, 5, and 5%, respectively (Figure S2B).

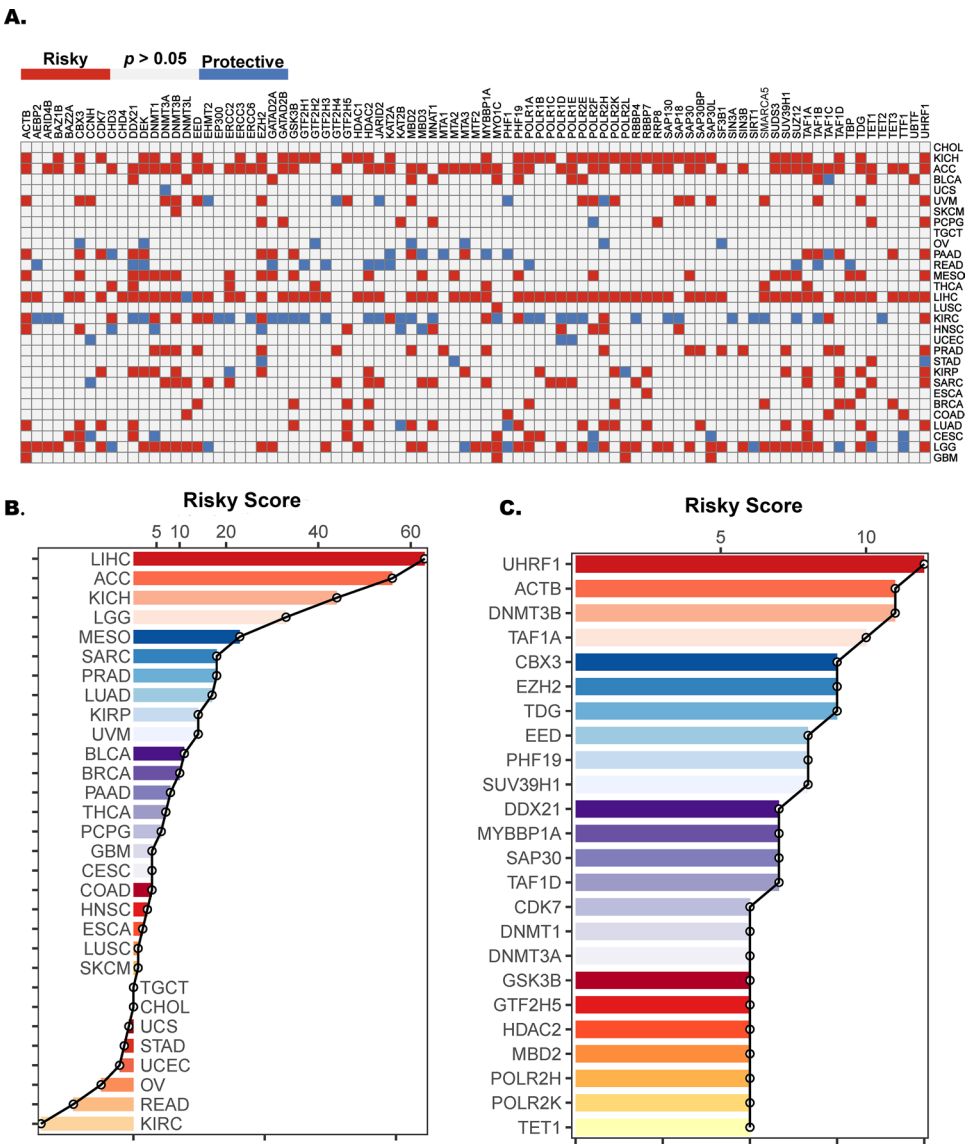

Fig. 1 Pancancer univariate Cox regression analysis. **A**. Summary of the correlations between epigenetic regulation relative genes expression and patient prognosis calculated by univariate Cox regression analysis. Red and blue represent epigenetic regulation relative genes expression significantly associated with worse survival and better survival, respectively. Only *P* values < 0.05 are shown. **B**. The risky score of each cancer. The risky score of each cancer was the total cox score of all the epigenetic regulation relative genes. **C**. The risky score of e ach gene. The risky score of each gene was the total cox score of each gene across different cancer types

3.2 Epigenetic score was a good indicator of patient prognosis in LIHC

As LIHC has the highest risky score across different cancer types, the next analysis was focus on LIHC (Fig. 1B). In order to better carry out futher research of epigenetic regulation related genes in LIHC, the independent risk factors among all the epigenetic regulation related genes of LIHC were screened using univariate and multivariate logistic regression analyses (Table 1). Multivariate logistic regression analysis indicated that the 23 genes were the independent risk factors in LIHC, which were listed in Table S4.

To further investigate the role of epigenetic regulation related genes in malignant progression of LIHC. Epigenetic score was defined based on the enrichment score (ES) of the 23 independent risk factors in LIHC, calculated by ssGSEA. Epigenetic score was significantly higher in tumor rather than normal tissue across different cancers (Fig. 3A). On the other hand, overall survival (Figs. 3B and S2A) and disease free survival (Figs. 3C and S2B) between high- Epigenetic score and low- Epigenetic score groups according to the median Epigenetic score cutoff value were analyzed via Kaplan–Meier survival analysis. We found that the patients with high Epigenetic score had significantly poorer prognosis than those with low Epigenetic score in LIHC, LUAD, KIRC, COAD, KICH, and PRAD. Besides, the disease free survival (DSS) between high and low Epigenetic score group were significantly in LIHC, KIRP, LUAD, THCA, KIRC, COAD, KICH, and PRAD.

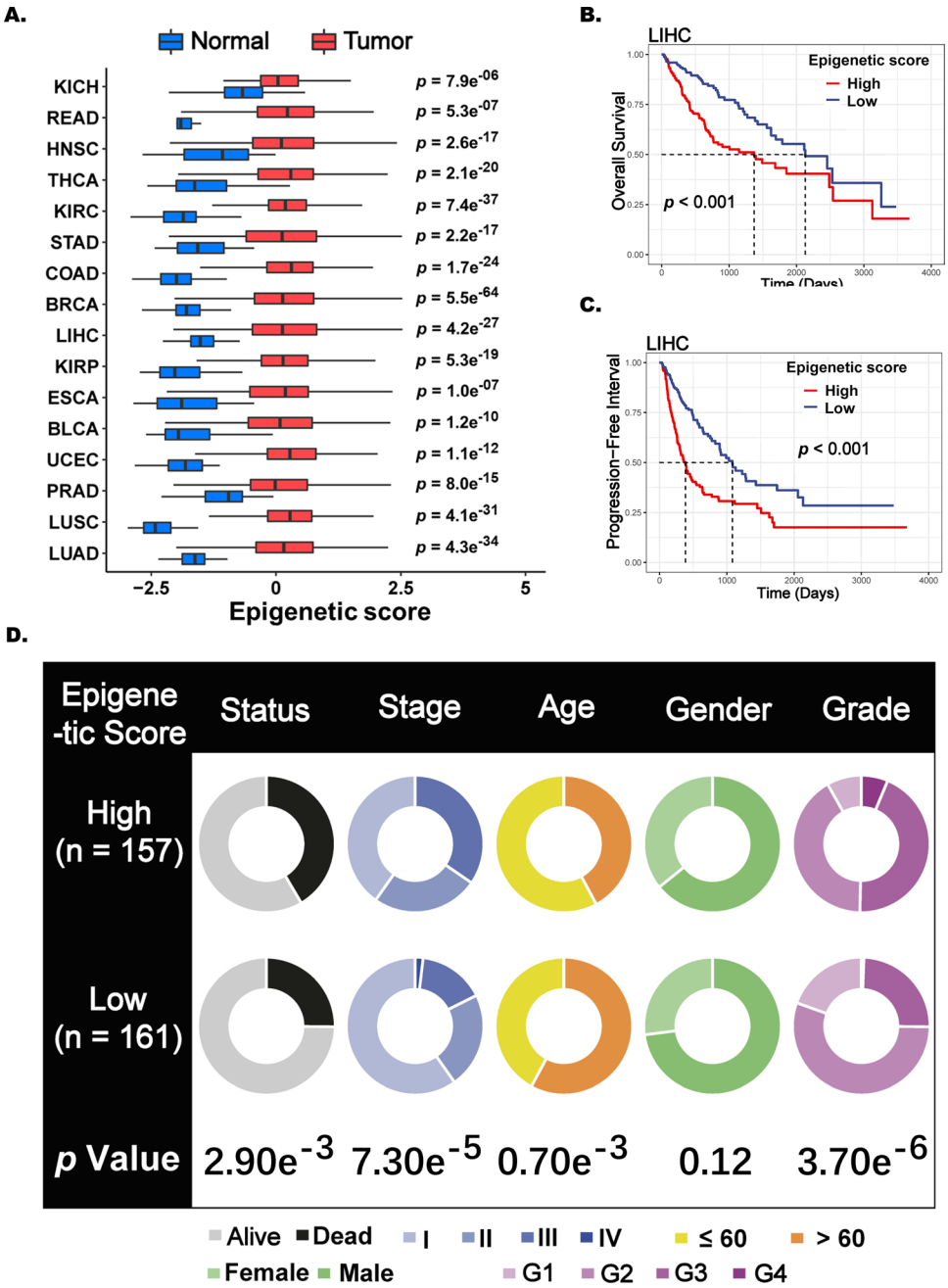

Fig. 2 The relations between Epigenetic score and patient histological sample and prognosis among Cancers. **A**. Differential Epigenetic score between cancer and normal tissue among cancers. **B**, **C**. Kaplan–Meier survival analysis between high- Epigenetic score and low- Epigenetic score groups according to the median Epigenetic score cut-off value. (GEO database). **D**. The relevance between Epigenetic score and phenotype of LIHC from TCGA dataset was verified by fisher exact test

Besides, we also investigate the clinical factors that might impact Epigenetic score. The Fisher's test showed that high Epigenetic score was positively associated with poor overall survival, higher tumor stage, younger age and higher propensity for high tumor Grade (Fig. 3D).

These founding indicate that Epigenetic score was particularly important in LIHC tumorigenesis and progressing.

3.3 Association between epigenetic score and tumor pathways in LIHC

To determine the underlying mechanism of epigenetic regulation related genes in malignant progressing, we performed tumor pathway analysis.

GSVA was performed to assess the pathway activities between high and low epigenetic score group divided by the epigenetic score median. As shown in Fig. 4, epigenetic score was positively correlated to MYC_TARGETS_V2, MYC_TARGETS_V1, MITOTIC_SPINGLE, G2M_CHECKPOINT, E2F_TARGETS and DNA_REPAIR pathway.

Table 1 Univariate and multivariate logistic regression

	Univariate analysis		Multivariate analysis	
	OR (95% CI)	P value	OR (95% CI)	P value
RBBP4	1.012 (1.004-1.021)	0.005	1.096 (1.042-1.153)	0.000
TAF1A	1.097 (0.938-1.283)	0.246		
TAF1B	1.216 (1.080-1.369)	0.001	1.005 (1.002-1.008)	0.001
DNMT3A	1.060 (1.018-1.103)	0.005	1.096 (1.042-1.153)	0.000
TET3	1.186 (0.978-1.439)	0.082		
POLR1A	1.083 (0.971-1.208)	0.153		
GSK3B	1.057 (1.019-1.097)	0.003	1.005 (1.002-1.008)	0.001
POLR2H	1.019 (1.010-1.029)	<0.001	1.096 (1.042-1.153)	0.000
SMARCA5	1.026 (0.988-1.065)	0.182		
SAP30	1.118 (1.053-1.186)	<0.001	1.005 (1.002-1.008)	0.001
CDK7	1.035 (1.002-1.070)	0.040	1.096 (1.042-1.153)	0.000
SAP30L	1.026 (1.006-1.046)	0.009	1.005 (1.002-1.008)	0.001
DEK	1.008 (0.998-1.017)	0.109		
HDAC2	1.025 (1.010-1.040)	0.001	1.096 (1.042-1.153)	0.000
GTF2H5	0.958 (0.839-1.095)	0.530		
ACTB	1.000 (1.000-1.001)	0.020	1.005 (1.002-1.008)	0.001
CBX3	1.011 (1.004-1.018)	0.001	1.096 (1.042-1.153)	0.000
EZH2	1.102 (1.049-1.158)	<0.001	1.005 (1.002-1.008)	0.001
POLR2K	1.003 (0.996-1.011)	0.371		
PHF19	1.040 (1.017-1.064)	<0.001	1.096 (1.042-1.153)	0.000
TET1	3.162 (1.350-7.406)	0.008	1.005 (1.002-1.008)	0.001
DDX21	1.023 (0.994-1.053)	0.121		
POLR2L	1.006 (1.003-1.009)	<0.001	1.096 (1.042-1.153)	0.000
RRP8	1.106 (1.055-1.159)	<0.001	1.005 (1.002-1.008)	0.001
EED	1.062 (1.007-1.120)	0.028	1.096 (1.042-1.153)	0.000
TAF1D	1.008 (0.999-1.018)	0.091		
TDG	1.058 (0.998-1.122)	0.059		
SUDS3	1.064 (0.996-1.137)	0.065		
MNAT1	1.020 (0.984-1.057)	0.281		
MYO1C	1.009 (0.998-1.019)	0.100		
MYBBP1A	1.020 (0.993-1.048)	0.151		
SAP30BP	1.021 (1.010-1.033)	<0.001	1.005 (1.002-1.008)	0.001
MBD2	1.013 (1.001-1.026)	0.041	1.096 (1.042-1.153)	0.000
POLR2E	1.007 (1.003-1.011)	0.001	1.005 (1.002-1.008)	0.001
UHRF1	1.049 (1.008-1.092)	0.018	1.096 (1.042-1.153)	0.000
DNMT1	1.023 (1.006-1.040)	0.009	1.005 (1.002-1.008)	0.001
DNMT3B	1.262 (0.998-1.596)	0.052		
RBBP7	1.013 (1.005-1.020)	0.001	1.096 (1.042-1.153)	0.000
SUV39H1	1.054 (0.994-1.117)	0.080		

OR, odds ratio; CI, confidence interval; NA, not available.

We downloaded the ssGSEA results for 1387 PARADIGM pathways and divided the samples into two groups according to their median epigenetic scores. Using the limma R package, differential pathway enrichment between high and low epigenetic score groups was analyzed, and the results are shown in Table S5 and Fig. 4A. Using the R package ggplot, immune-related pathways were visualized. According to the results shown in Fig. 4B, immunosuppressive pathways, such as IL2, IL4 and FGFR2 related pathway, are prominently enriched in the high epigenetic score group, suggesting that epigenetic pathway activation could be associated with LIHC development and immune tolerance. And from GO enrichment, it also indicated that high epigenetic score was closely related to receptor ligand activity,signaling receptor

Fig. 3 Functional implications of elevated epigenetic score in LIHC. Enrichment analysis for elevated epigenetic score and tumor hallmark pathway. NES is the normalized enrichment score in the GSEA algorithm

activator activity, antigen binding, cytokine activity and immunoglobulin receptor binding, which may affect the immune microenvironment (Fig. 4C). Therefore, we further investigated the correlation between epigenetic score and immunity cycle. We found that epigenetic score was significantly associated with release of cancer antigens, Th22 cell recruiting, B cell recruiting, infiltration of T cells into tumors, recognition of cancer cells by T cells and Killing of cancer cells (Fig. 4D).

Together, the above results demonstrate a highly probability of the positive correlation between immune evasion and epigenetic score.

3.4 Systematic analysis of immunomodulatory crosstalk between UHRF1 and immune evasion

From the above analysis, we found that UHRF1 was differentially expressed in LIHC (Fig. 2A) and has the highest risky score (Fig. 1C), which indicated that UHRF1 may play an important role in LIHC malignant progressing. Besides, we comprehensively analyze the spatial heterogeneity of UHRF1 expression from different region of HCC patients. As shown in Fig. 5, UHRF1 expression level gradually increases in normal tissues, eading-edge area of tumor, and tumor tissues. Moreover, in tumor tissues, those area with high proportion of malignant cells had higher UHRF1 expression level (Fig. 6), which emphasized again that UHRF1 may plays an important role in HCC.Therefore, we further

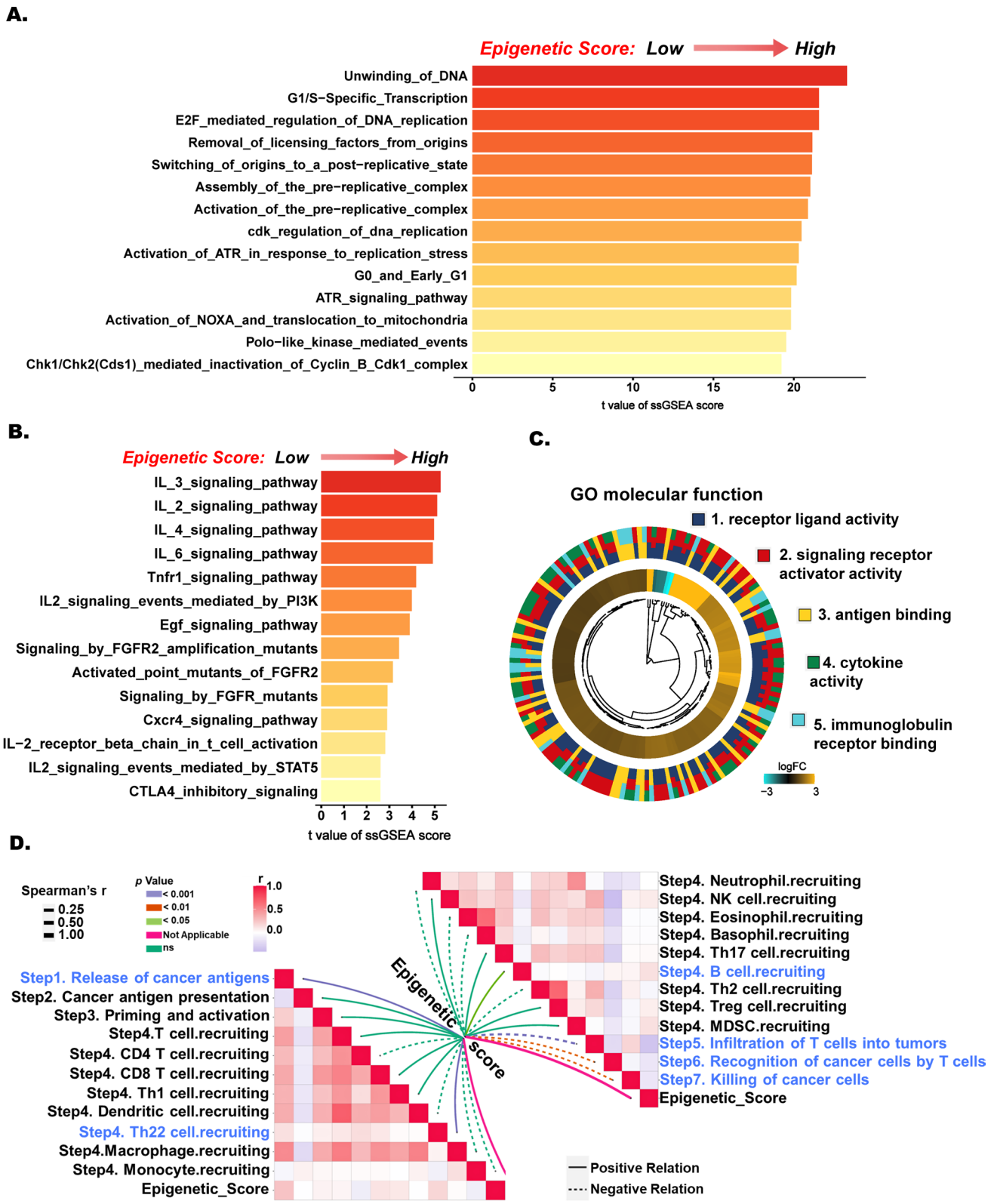

Fig. 4 Pathway enrichment of elevated epigenetic score in LIHC. **A**. Comparison of ssGSEA score for constituent PARADIGM algorithm integrates pathway between high and low Epigenetic score groups according to the median Epigenetic score cutoff value. **B**. Comparison of ssGSEA score for constituent PARADIGM algorithm integrates immune-related pathway between high and low Epigenetic score groups according to the median epigenetic score cutoff value. **C**. GO enrichment of high epigenetic score group (versus low Epigenetic score group). **D**. Correlation between epigenetic score and immunity cycle related pathway. The blue label text represent the pathways significantly associated with epigenetic score (*P* values < 0.05)

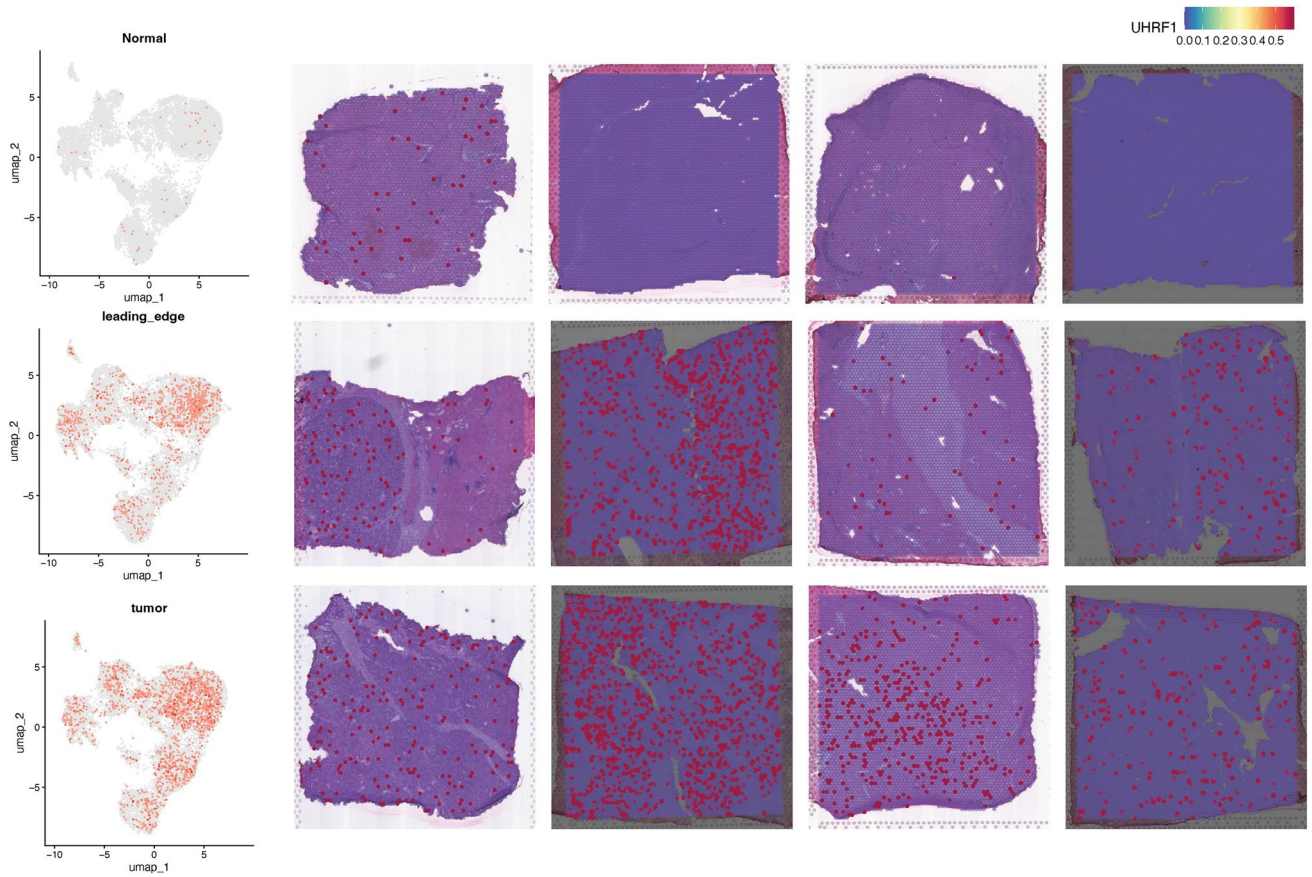

Fig. 5 UHRF1 expression in LIHC. Comparison of UHRF1 expression in different region of HCC patients. The first, second, and third rows represent the normal tissue, leading-edge area of tumor, and tumor tissue of the HCC patient, respectively. Slices in the same column come from the same patient

investigated the relation between the immunity and UHRF1 expression in LIHC. From GSVA analysis results, we found that UHRF1 expression was positively correlated to MYC_TARGETS_V2, MYC_ TARGETS_V1, MTORC1_SIGNALING, MITOTIC_SPINGLE, G2M_.

CHECKPOINT, E2F_TARGETS and DNA_REPAIR pathway (Fig. 7).

To further investigate the immune landscape differences according to the UHRF1 expression, single cell RNA sequencing (scRNA-seq) atlas from GSE156625 was used. We identified 8 major cell types of the HCC samples as shown in the Louvain clustering map (Fig. 8A), and we found that UHRF1 was mainly expressed in hepatocytes, macrophage, NK_Cells (Fig. 8B). In order to better study the effect of different UHRF1 expression levels on cell communication in tumor microenvironment, HCC patients were divided into two groups according to UHRF1 expression. From Fig. 8C, it's easily discovered that these patients were belong to high UHRF1 expression group, including P1, P2, P5, P7, P9, P11, P15, while the rest patients were belong to low UHRF1 expression group, including P3, P4, P6, P8, P10, P13, P14. To decipher the cell–cell interaction interactions in different UHRF1 level, we performed Cellchat analysis which indicated that patients with higher UHRF1 expreesion level exhibited more stronger interaction between HCC hepatocytes and the cells including the macrophage, NK cells, Tregs and endothelial cells (Fig. 8D). Futhermore, from the overall signaling pattern analysis of HCC patients (Fig. 8E), we found that macrophage and endothelial cells were the dominant mediator and influencer, suggesting their role were significant impacted by the expression level of UHRF1. Compared to other signaling, MHC-II, COLLAGEN, CXCL, FN1, SPP1, NOTCH, VEGF and etc. were noticeably stronger in higher UHRF1 expression patients. Besides, differential expression analysis was performed and we found that SPP1 was remarkably higher in macrophage of patients with high UHRF1 expression (log2FC = 3.18, *P* value = $8.32E^{-96}$), which was shown in Fig. 8G and Table S6. Finally, TIDE algorithm was performed and as shown in Fig. 8H and Table S7, the response rate of immunotherapy in low UHRF1 expression group (58.1%,) was significantly higher than that in high UHRF1 expression group (41.9.3%).

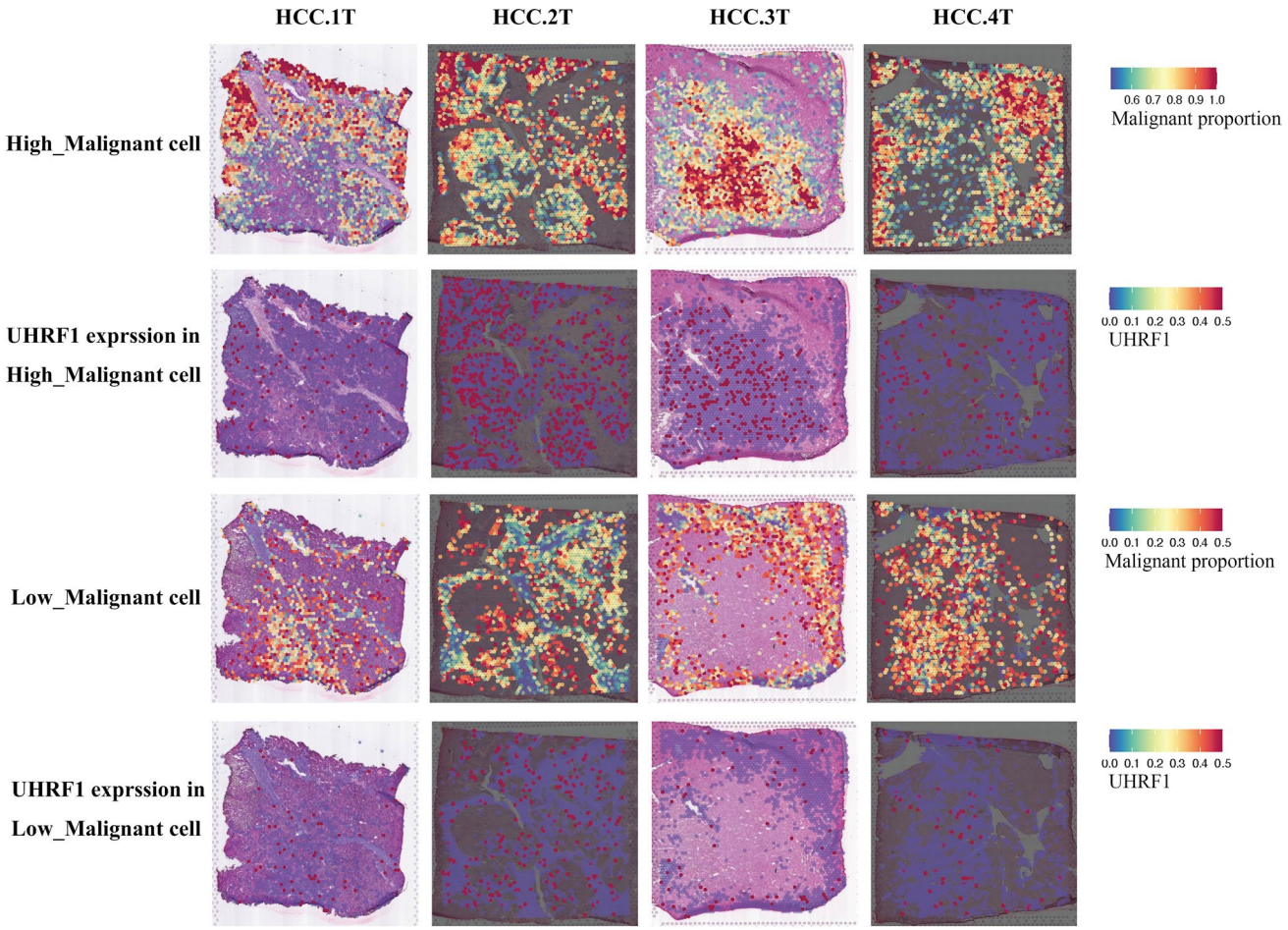

Fig. 6 UHRF1 expression in LIHC. Comparison of UHRF1 expression in different region of HCC tumor tissue. High_ malignant cell was defined as the proportion of malignant cells were over than 50%. Low_ malignant cell was defined as the proportion of malignant cells were less than 50%

3.5 Virtual screening to find potential pharmacological intervention towards UHRF1

From the above evidence, UHRF1 appears to be an appealing target for unique or adjuvant antitumor pharmaceutical therapies. Therefore, we screened natural compound libraries for potential pharmacological interventions against UHRF1. The top 20 compounds with the highest docking scores are listed in Supplemental File 3. As shown in Fig. 9, salvianolic acid B, safflower yellow, pentagalloylglucose, sennoside B, cefpiramide sodium, and chicoric acid had the highest docking scores, suggesting that these compounds might be good candidates for LIHC remedies.

4 Discussion

Aberrant epigenetic status bring abnormal transcriptional variation which accelerating the occurrence and development of tumors [13], and subsequently leading to the acquiring of immune evasion properties that was involved in the resistance to immunotherapy [14]. Besides, previous study also identified that epigenetic reprogramming was emerging as a the initiator of evil of multiple malignant progression of tumors including haywire proliferation, vascularization, epithelial-mesenchymal transition (EMT) and metastasis [14]. To futher investigated the role of epigenome in tumor malignant progress, we first performed a pancancer analysis of all the epigenetic regulation related

Fig. 7 Functional implications of elevated UHRF1 expression in LIHC. Enrichment analysis for elevated epigenetic score and tumor hallmark pathway. NES is the normalized enrichment score in the GSEA algorithm

genes abtained from GSEA online website and found that most of them were up regulated and participated in the malignant progress of most cancers,especially in HCC.

To futher revealed the global alterations of the epigenome at genetic landscape, we used ssGSEA to process pan-cancer expression data to establish epigenetic score to characterize epigenome status across different tumor types and addressed which genetic and clinincal factors were related to the dysregulation of the epigenome. Herein, we found that epigenetic score was elevated across different cancers and further supported the previous research which proposing epigenome as a hallmark of tumors [15]. Interestingly, we observed that epigenetic score remarkably reinforced in HCC and closely related to poor prognosis of these patients.

Previous study had been reported that epigenetic aberrations were strong malignant triggers and were commonly observed in HCC [16–19]. It could facilitated tumorigenesis through various way including metabolic regulation, EMT induction and driving immune escape and drug resistance [20, 21]. From our analysis, we confirmed that epigenetic aberrations were closely related to abnormal cell cycle, immune resistance and immune cycle aberration, which indicated that further research is needed to provide updated recommendations on the treatment of HCC based on comprehensive evidence from multiple sources.

More and more evidence validates that matching a drug to a specific targets could be an effective way on the potential for durable clinical benefit [22]. Herein, we found that UHRF1 was upregulated in most cancers and could served

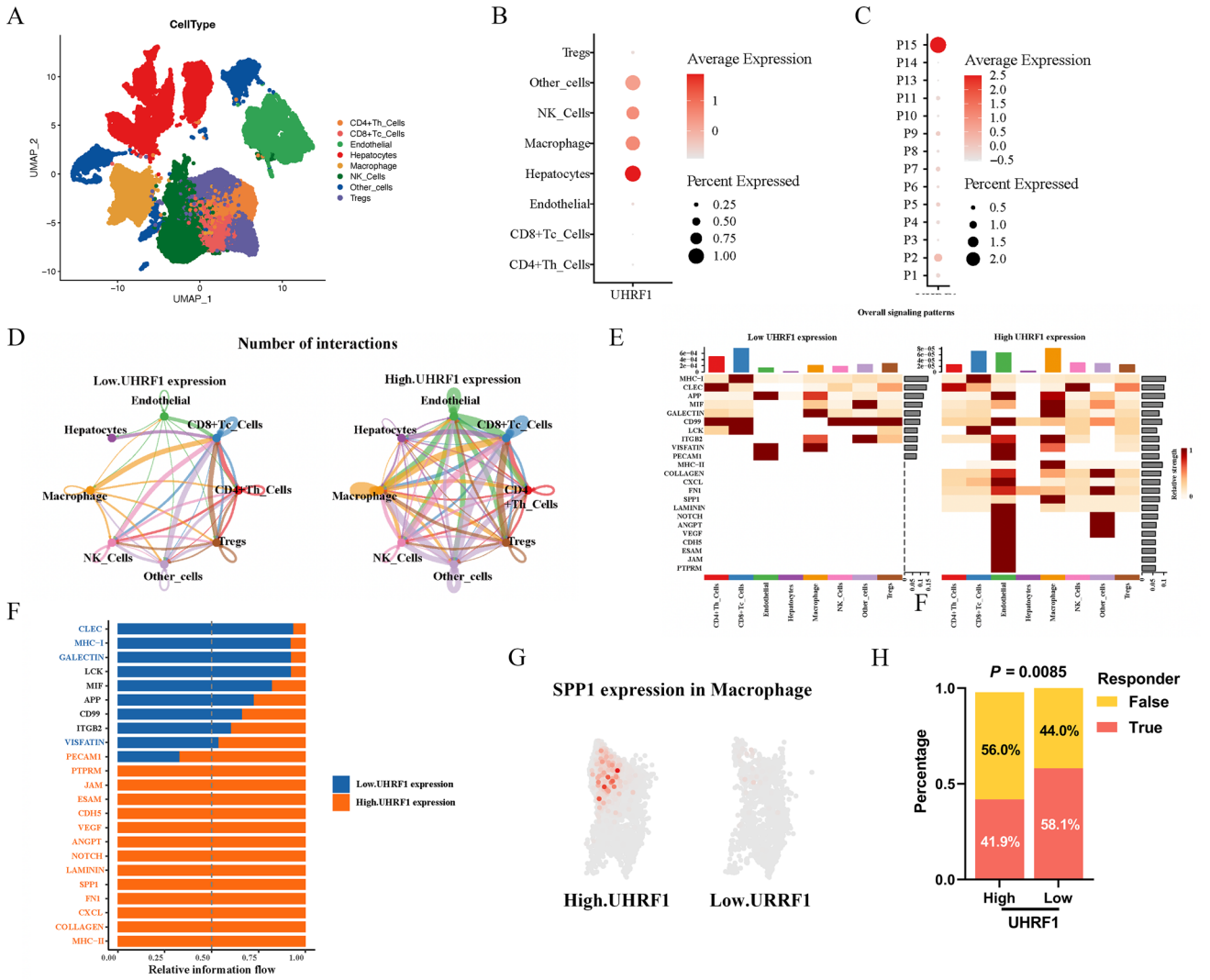

Fig. 8 Immune landscape and distinct genomic profiles associated with UHRF1 expression in single cell landscape. **A**. 8 mega-clusters identified from scRNA-seq obtained from GSE156625 datasets. **B**. UHRF1 expression of different cell type in HCC. **C**. UHRF1 expression of 14 HCC patients from scRNA-seq library. **D**. Interaction plot and intercellular communication networks for different cell types from low UHRF1 expression and high UHRF1 expression. The thicker line and the more numbers represented the stronger interaction among the two cell types. **E**. Comparison of tumor signaling patterns between low UHRF1 expression and high UHRF1 expression. The results were shown as a heatmap of tumor signaling pathways and the relative importance of each cell group based on the computed network centrality measures of signaling networks. **F**. Comparison of relative tumor signaling flow between low UHRF1 expression and high UHRF1 expression. **G**. SPP1 expression in macrophage according to the UHRF1 expression. **H**. Association of UHRF1 expression and the response to the immunosuppressive checkpoints therapy according to TIDE prediction.

as a prognostic factor across different cancer types. Consistent with our conclusion, it had been confirmed that UHRF1 served as an oncogene and epigenetic hallmark inducing global DNA hypomethylation of HCC and subsequently driving tumorigenesis [23]. As a well-known epigenetic regulator, UHRF1 has been implicated in the progression and prognosis of various solid tumors, including osteosarcoma, lung cancer, and breast cancer, highlighting its pathological significance. However, studies investigating the role of UHRF1 in HCC remain relatively limited [24]. Therefore, in order to better reveal the role of UHRF1 in tumorigenesis. We firsted employed pancancer pathway analysis of UHRF1 and found that UHRF1 expression was positively correlated to the pathways related to cell life cycle and damage repair. Similar to our analysis results, it had reported that particular inhibiting the UHRF1/BRCA1 protein complex significantly decreased tumor cell viability and led to cell apoptosis and DNA damage without detectable toxicity [25]. Besides, antecedent work showed that UHRF1 knockdown inhibited cell proliferation via the cell cycle modification [26]. At the same time, from previous study we found that UHRF1 had important implication for the modification of tumor immune microenvironment. circUHRF1 from HCC cells could upregulated the TIM-3 expression and thus inhibited NK cell-derived IFN-γ and TNF-α

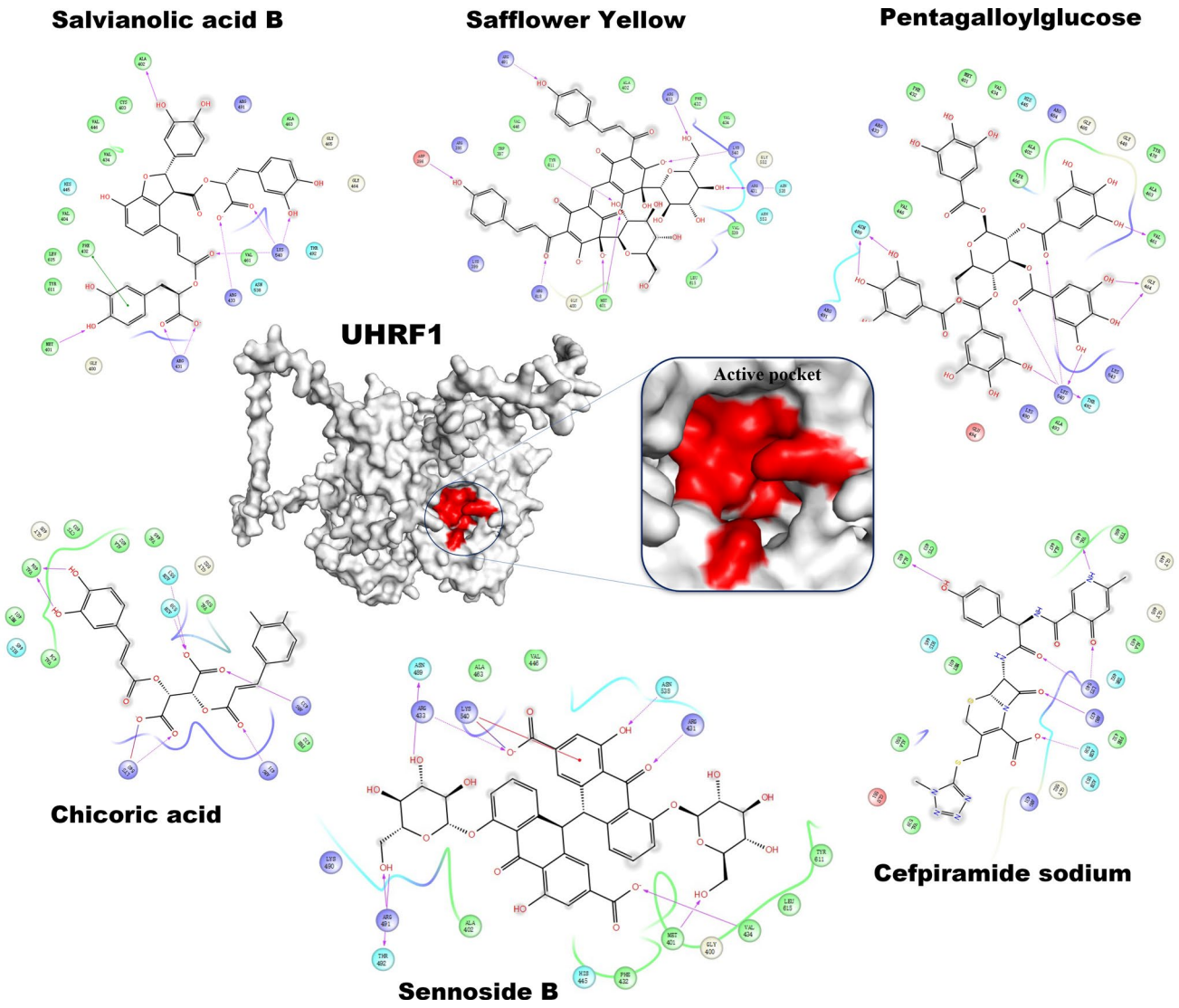

Fig. 9 Virtual screening to find potential pharmacological intervention towards UHRF1

secretion leading to the NK cell dysfunction [27]. Also, it had been detected that crosstalk between TAMs and HCC cells foster a self-enhancing oncogenic loop with an continuously robust TAM recruitment and activation forming an immunosuppressive microenvironmen [28].

As the important role of UHRF1 in tumor progression, we therefore employed an scRNA analysed to make an deep insight on the impact of UHRF1 on tumor immunity. In our study, we found that UHRF1 was strongly related to underlying molecular pattern of macrophage. Noticeably, we found that higher UHRF1 expression accompanied with a higher SPP1 expression in HCC patients. Previous study demonstrated that SPP1 was an strong oncogene implicated in multiple malignant process of HCC, including the promotion of PD-L1 expression, drug resistance, alternative activation of M2 macrophages and the facilitated effect on tumor migration and metastasis [29–31]. Besides, a spatial crosstalk between $SPP1^{+}$ macrophages and cancer-associated fibroblasts could leading to an immune restrictive effect and construted a tumour immune barrier to facilating tumor progress and affecting the anti-PD-1 treatment effitiency [32]. Finally, TIDE algorithm was employed to predict the immune checkpoint blockade response. We found that higher UHRF1expression generated poorer respond to immune checkpoint blockade which was consistent with the previous article mentioned before.

Taken together, targeted inhibition of UHRF1 would be a promising strategy to reverse the immune suppression state of LIHC, which indicated the important implications for the development and application of UHRF1 inhibitor. So, we performed virtual screening to find potential compounds targeting UHRF1. From the results, we found that several

natural compounds including salvianolic acid B, safflower yellow, pentagalloylglucose, sennoside B, cefpiramide sodium and chicoric acid could be potential for small-molecule inhibitors targeting UHRF1 which needed futher experimentation in the future. This study systematically integrates multi-omics data to define an innovative "Epigenetic Score," providing novel insights into the role of ERRGs in cancer progression, particularly in LIHC. Future research should focus on experimental validation of the Epigenetic Score and UHRF1's role in LIHC, as well as the development of targeted therapies, including the identified small-molecule inhibitors, to improve clinical outcomes.

In conclusion, we provided a conceptual framework to figure out the relationship between cancer epigenetics and the malignant toumr progression. In this perspective, our study will progressively support the development of new strategies to treat LIHC.

5 Limitation

As experimental validation has not yet been conducted at this stage and the work remains solely at the level of data analysis, this constitutes a limitation of the present study.

Acknowledgements Not applicable.

Author contributions Jiehua Zheng and Weixun Lin contributed equally to this work. Jiehua Zheng and Weixun Lin designed and performed the bioinformatics analysis. Data collection and first draft of the manuscript was written by Jiehua Zheng. Jing Tang provided advised on study design. Bo Xu advised on study design, supervised the data analysis, performed critical review of the manuscript and provided funding.

Funding This work was supported by Shantou Medical Science and Technology Planning Project (Grant Number 210625106490696).

Availability of data and materials All data of this article comes from public databases that is freely available. 148 epigenetic regulation related genes were obtained from reactome pathways (R-HSA-212165) which downloaded from website of Gene Set Enrichment Analysis (GSEA) (http://www.gseamsigdb.org/gsea/index.jsp). And 142 epigenetic regulation relative gene list (Table S1) were selected in our study (6 of the 148 genes are not in our pancancer expression matrix). The pancancer mRNA expression data and clinical data with follow-up were downloaded from National Cancer Institute Cancer Research Genomic Data Commons (GDC) (https://gdc.cancer. gov/about-data/publications/pancanatlas). CIBERSORT immune fractions and Scores for 160 Genes Signatures in Tumor Samples were downloaded from GDC (https://gdc.cancer.gov/about-data/ publications). The Cancer Genome Atlas (TCGA) LIHC Phenotypes data was obtained from xena website (https://xenabrowser.net/datapages/). The pan-cancer ssGSEA scores for 1387 constituent PARADIGM algorithm integrates pathway was obtained from xena website. The Gene Expression Omnibus (GEO) database (http://www.ncbi.nlm.nih.gov/geo/) was explored, and GSE14520 gene expression dataset was downloaded for this study. Mutation data of LIHC was downloaded from cBioPortal database (http://www.cbioportal.org /datasets). Gene expression profile of exosome was downloaded from BBcancer database (http://bbcancer.renlab.org/download).

Declarations

Ethics approval and consent to participate Not applicable.

Consent for publication We all agreed this article for publication.

Competing interests The authors declare no competing interests.

References

1. Abaza T, El-Aziz MKA, Daniel KA, Karousi P, Papatsirou M, Fahmy SA, Hamdy NM, Kontos CK, Youness RA. Emerging role of circular RNAs in hepatocellular carcinoma immunotherapy. Int J Mol Sci. 2023;24(22):16484. https://doi.org/10.3390/ijms242216484.
2. Eissa S, Swellam M, El-Mosallamy H, Mourad MS, Hamdy NM, Kamel K, Zaglol AS, Khafagy MM, El-Ahmady O. Diagnostic value of urinary molecular markers in bladder cancer. Anticancer Res. 2003;23(5b):4347–55.
3. Dawson MA, Kouzarides T. cancer epigenetics: from mechanism to therapy[J]. Cell. 2012;150(1):12–27.

4. Ilango S, Paital B, Jayachandran P, et al. Epigenetic alterations in cancer[J]. Front Biosci. 2020;25(6):1058–109.
5. Garcia-Martinez L, Zhang Y, Nakata Y, et al. Epigenetic mechanisms in breast cancer therapy and resistance[J]. Nat Commun. 2021;12(1):1786.
6. Shah K, Rawal RM. Genetic and epigenetic modulation of drug resistance in cancer: challenges and opportunities[J]. Curr Drug Metab. 2019;20(14):1114–31.
7. El Mesallamy HO, Rashed WM, Hamdy NM, Hamdy N. High-dose methotrexate in Egyptian pediatric acute lymphoblastic leukemia: the impact of ABCG2 C421A genetic polymorphism on plasma levels, what is next? J Cancer Res Clin Oncol. 2014;140(8):1359–65. https://doi.org/10.1007/s00432-014-1670-y.
8. Miranda FC, Dos SLM, Silva SR, et al. Epidrugs: targeting epigenetic marks in cancer treatment[J]. Epigenetics. 2019;14(12):1164–76.
9. Tomasi TB, Magner WJ, Khan AN. Epigenetic regulation of immune escape genes in cancer[J]. Cancer Immunol Immunother. 2006;55(10):1159–84.
10. Montenegro MF, Sanchez-Del-Campo L, Fernandez-Perez MP, et al. Targeting the epigenetic machinery of cancer cells[J]. Oncogene. 2015;34(2):135–43.
11. Ali NA, Hamdy NM, Gibriel AA, El Mesallamy HO. Investigation of the relationship between CTLA4 and the tumor suppressor RASSF1A and the possible mediating role of STAT4 in a cohort of Egyptian patients infected with hepatitis C virus with and without hepatocellular carcinoma. Arch Virol. 2021;166(6):1643–51. https://doi.org/10.1007/s00705-021-04981-8.
12. Youssef SS, Hamdy NM. SOCS1 and pattern recognition receptors: TLR9 and RIG-I; novel haplotype associations in Egyptian fibrotic/cirrhotic patients with HCV genotype 4. Arch Virol. 2017;162(11):3347–54. https://doi.org/10.1007/s00705-017-3498-7.
13. Hogg SJ, Beavis PA, Dawson MA, Johnstone RW. Targeting the epigenetic regulation of antitumour immunity. Nat Rev Drug Discov. 2020;19(11):776–800. https://doi.org/10.1038/s41573-020-0077-5.
14. Liu S, Sun Q, Ren X. Novel strategies for cancer immunotherapy: counter-immunoediting therapy. J Hematol Oncol. 2023;16(1):38. https://doi.org/10.1186/s13045-023-01430-8.
15. Pastushenko I, Brisebarre A, Sifrim A, Fioramonti M, et al. Identification of the tumour transition states occurring during EMT. Nature. 2018;556(7702):463–8. https://doi.org/10.1038/s41586-018-0040-3.
16. Flavahan WA, Gaskell E, Bernstein BE. Epigenetic plasticity and the hallmarks of cancer. Science. 2017;357(6348):eaal2380. https://doi.org/10.1126/science.aal2380.
17. El-Mesallamy HO, Hamdy NM, Rizk HH, El-Zayadi AR. Apelin serum level in Egyptian patients with chronic hepatitis C. Med Inflamm. 2011;2011:703031. https://doi.org/10.1155/2011/703031.
18. Hammad R, Eldosoky MA, Elmadbouly AA, Aglan RB, AbdelHamid SG, Zaky S, Ali E, Abd El Hakam FE, Mosaad AM, Abdelmageed NA, Kotb FM, Kotb HG, Hady AA, Abo-Elkheir OI, Kujumdshiev S, Sack U, Lambert C, Hamdy NM. Monocytes subsets altered distribution and dysregulated plasma hsa-miR-21–5p and hsa-miR-155–5p in HCV-linked liver cirrhosis progression to hepatocellular carcinoma. J Cancer Res Clin Oncol. 2023;149(17):15349–64. https://doi.org/10.1007/s00432-023-05313-w.
19. Hammad R, Aglan RB, Mohammed SA, Awad EA, Elsaid MA, Bedair HM, Khirala SK, Selim MA, Abo Elqasem AA, Rushdi A, Ali M, Abo-Elkheir OI, Sanad EF, Hamdy NM. Cytotoxic T cell expression of leukocyte-associated immunoglobulin-like receptor-1 (LAIR-1) in viral hepatitis c-mediated hepatocellular carcinoma. Int J Mol Sci. 2022;23(20):12541. https://doi.org/10.3390/ijms232012541.
20. Nagaraju GP, Dariya B, Kasa P, Peela S, El-Rayes BF. Epigenetics in hepatocellular carcinoma. Semin Cancer Biol. 2022;86(Pt3):622–32. https://doi.org/10.1016/j.semcancer.2021.07.017.
21. Wei Y, Tang X, Ren Y, Yang Y, et al. An RNA-RNA crosstalk network involving HMGB1 and RICTOR facilitates hepatocellular carcinoma tumorigenesis by promoting glutamine metabolism and impedes immunotherapy by PD-L1+ exosomes activity. Signal Transduct Target Ther. 2021;6(1):421. https://doi.org/10.1038/s41392-021-00801-2.
22. Lu M, Zhu WW, Wang X, Tang JJ, et al. ACOT12-dependent alteration of acetyl-CoA drives hepatocellular carcinoma metastasis by epigenetic induction of epithelial-mesenchymal transition. Cell Metab. 2019;29(4):886-900.e5. https://doi.org/10.1016/j.cmet.2018.12.019.
23. Hollingsworth SJ. Precision medicine in oncology drug development: a pharma perspective. Drug Discov Today. 2015;20(12):1455–63. https://doi.org/10.1016/j.drudis.2015.10.005.
24. Kim A, Benavente CA. Oncogenic roles of UHRF1 in cancer. Epigenomes. 2024;8(3):26. https://doi.org/10.3390/epigenomes8030026.
25. Mudbhary R, Hoshida Y, Chernyavskaya Y, et al. UHRF1 overexpression drives DNA hypomethylation and hepatocellular carcinoma. Cancer Cell. 2014;25(2):196–209. https://doi.org/10.1016/j.ccr.2014.01.003.
26. Yin L, Liu Y, Peng Y, et al. PARP inhibitor veliparib and HDAC inhibitor SAHA synergistically co-target the UHRF1/BRCA1 DNA damage repair complex in prostate cancer cells. J Exp Clin Cancer Res. 2018;37(1):153. https://doi.org/10.1186/s13046-018-0810-7.
27. Wan X, Yang S, Huang W, et al. UHRF1 overexpression is involved in cell proliferation and biochemical recurrence in prostate cancer after radical prostatectomy. J Exp Clin Cancer Res. 2016;35:34. https://doi.org/10.1186/s13046-016-0308-0.
28. Zhang PF, Gao C, Huang XY, et al. Cancer cell-derived exosomal circUHRF1 induces natural killer cell exhaustion and may cause resistance to anti-PD1 therapy in hepatocellular carcinoma. Mol Cancer. 2020;19(1):110. https://doi.org/10.1186/s12943-020-01222-5.
29. Zhang J, Zhang H, Ding X, Hu J, et al. Crosstalk between macrophage-derived PGE2 and tumor UHRF1 drives hepatocellular carcinoma progression. Theranostics. 2022;12(8):3776–93. https://doi.org/10.7150/thno.69494.
30. Zhu Y, Yang J, Xu D, et al. Disruption of tumour-associated macrophage trafficking by the osteopontin-induced colony-stimulating factor-1 signalling sensitises hepatocellular carcinoma to anti-PD-L1 blockade. Gut. 2019;68(9):1653–66. https://doi.org/10.1136/gutjnl-2019-318419.
31. Eun JW, Yoon JH, Ahn HR, et al. Cancer-associated fibroblast-derived secreted phosphoprotein 1 contributes to resistance of hepatocellular carcinoma to sorafenib and lenvatinib. Cancer Commun. 2023;43(4):455–79. https://doi.org/10.1002/cac2.12414.
32. Liu Y, Xun Z, Ma K, et al. Identification of a tumour immune barrier in the HCC microenvironment that determines the efficacy of immunotherapy. J Hepatol. 2023;78(4):770–82. https://doi.org/10.1016/j.jhep.2023.01.011.